Hindawi
International Transactions on Electrical Energy Systems
Volume 2023, Article ID 1464297, 17 pages
https://doi.org/10.1155/2023/1464297

Research Article

Two Decentralized Dynamic State Estimation Schemes for Multimachine Power Systems with Transmission Losses

Natanael Vieyra,[1] **Paul Maya-Ortiz**,[2] **and César Angeles-Camacho**[1]

[1]*Engineering Institute, National Autonomous University of Mexico (UNAM), 04510 Ciudad de México, Mexico*
[2]*Department of Control and Robotics, National Autonomous University of Mexico (UNAM), 04510 Ciudad de México, Mexico*

Correspondence should be addressed to Natanael Vieyra; nvieyrav@iingen.unam.mx

Received 26 September 2022; Revised 31 December 2022; Accepted 10 January 2023; Published 3 February 2023

Academic Editor: Yu-Chi Wu

This article addresses the problem of estimating the state of a multimachine power system (MPS). To work with power networks with lossy transmission lines, a variation of the classical third-order MPS is proposed by considering generators' electrical power injected into the grid as a state variable. Based on a linear decentralized estimation model (tailored for a specific purpose), the state variables of generators (load angle, relative speed, and electrical power) together with terminal voltage magnitudes are estimated in a decentralized fashion through two new robustly convergent linear Luenberger estimators, one based on load angle measurement and the other based on relative speed measurement. The new MPS estimation model includes a set of robustly quick observable states, one per machine, which allows capturing the interaction with other generators, transmission line losses, unknown disturbances, and model errors. The result is a design superior to other related estimation techniques such as the extended Kalman filter (EKF) or Sliding Modes Perturbation Observer (SMPO) in terms of (i) a conventional-like simple pole placement-based tuning, (ii) low online computational load and disturbance rejection capability, and (iii) small gain-based convergence assessment. The performance of the proposed state estimation scheme is illustrated in a 3-machine power system under different operational conditions.

1. Introduction

Multimachine power systems (MPSs) are one of the most representative examples of large-scale interconnected systems. An MPS comprises a set of generators (which have pretty different inertia constants) and loads interconnected through transmission lines. The main objective is to generate, transform, distribute, and consume electrical energy [1, 2].

The MPS functioning may be affected by different disturbances, e.g., three-phase faults, load variations, and parameter uncertainty. Thus, different control approaches have been proposed to ensure optimal operating conditions [3–6]. However, these control schemes regularly assume the full knowledge of system state variables through sensors, an unnatural assumption due to physical and economic conditions. Therefore, despite the improved quality of the measurement devices, it is always necessary to count on a suitable tool to deliver information about the system when required. Therefore, a state estimator (SE) is a helpful tool for monitoring and controlling electrical networks.

Dynamic system state estimators developed decades ago, and different local and centralized schemes are found in scientific literature, many of which are based on the Extended Kalman (EKF) approach [7–14] and some of its variants [15–22]. Despite its robust performance (in the presence of parametric errors and measurement noise) and well-known constructive design, these dynamic estimators have a heuristic tuning, not to mention the lack of formal robust convergence proofs. Also, for those designed under a centralized approach (*Wide-Area*) [7, 14, 21], there is a heavy computational load associated with integrating a set of nonlinear (NL) ordinary differential equations (ODEs) (in a number that grows quadratically with the number of states). In contraposition, the NL sliding mode perturbation observer (SMPO) [23] is built based on a decentralized model variant of the NL MPS model, with additional (called fictitious) states that account for intermachine state interaction. The NL SMPO has an efficient computational load (as the number of ODEs to be integrated grows linearly with the number of states) and formal robust convergence proof. However, the SMPO presents a complex structure, unclear tuning, and fragility to noisy measurements.

Along with the estimation schemes mentioned above, Luenberger-like observers can also be found in scientific literature [24–26]. In [24, 25], the estimator design is based on the fully linearized representation of the MPS, ignoring the model errors. On the contrary, by employing a linear representation of MPS, the state vector is reconstructed through a centralized approach [26]. However, the observer gains are precalculated offline around a particular equilibrium point.

Our work is the natural extension of [27]; for the lossless MPS system, we proposed a decentralized dynamic estimator based on load angle measurement that retains the advantages of the EKF and SMPO observers and overcomes their obstacles. In the present work, to be more practical, we have considered an MPS with lossy transmission lines through a comprehensive modeling approach, demonstrating that this assumption does not modify the conceptual idea behind the decentralized estimation methodology. The present study also includes designing a decentralized dynamic state estimator based on the relative speed measurement and a method focused on estimating the terminal voltage magnitudes from estimated state variables. In summary, the decentralized reconstruction of the state vector associated with each generator (load angle, relative speed, electrical power, and terminal voltage magnitudes) is carried out through two linear (L) decentralized (D) geometric estimators (GEs) (Luenberger-like observer) [28–30], one through employing the load angle as measured output and the other one based on the relative speed measurement. The proposed state estimation methodology (which also includes the construction of a tailored estimation model) is a point of departure to address the observer-based output-feedback control design problem with an application-oriented robust decentralized scheme. The developed methodology might be a novel alternative to those control approaches based on Lyapunov-like methods. Specifically, because these control schemes require the construction of Lyapunov functions, which for transmission systems with medium-length transmission line models (transfer conductances between buses) is not a trivial task [31–33].

Firstly, the conventional NL-centralized (NL-C) model of the MPS (classical third-order dynamic model) is rewritten so that the electrical power injection of generators is a new state variable to include the transmission lines' losses effect on the generator dynamics. In addition, the new NL-C MPS model is realized as a set of linear (L) decentralized (D) robustly observable models with augmented states that capture nonlinearity, parameter error, transmission line losses, and intermachine state interaction. Furthermore, either based on load angle or relative speed measurements (which is an advantage in the case that load angles of generators are not available as measurements [34, 35]), two linear geometric (Luenberger-like) observers with linear-decentralized measurement injection are built on the basis of the robust observability property of the linear model tailored for the estimation purpose at hand [28–30]. Then, the robust functioning of both estimators is assured with conditions coupled with a conventional-like tuning scheme. Finally, the proposed estimation methodology is illustrated and tested with a representative benchmark example employed in previous MPS studies [4, 5, 36, 37], finding that the proposed estimator yields a robust performance against modeling and measurement errors.

2. Problem Formulation

In this section, the classical third-order MPS dynamic model is rewritten by considering the electrical power injected by generators into the grid as a state variable instead of using generators' traditional transient internal voltages as one of them. Then, the estimation objective is presented.

2.1. A Variant of the Multimachine Power System Model. The dynamic behavior of a large-scale MPS, which consists of N synchronous generators interconnected through lossy power lines, is represented by

$$\dot{\delta}_i = \omega_i, \delta_i(0) = \delta_{i0}, \tag{1a}$$

$$\dot{\omega}_i = -\frac{D_i}{2H_i}\omega_i + \frac{1}{2H_i}\left(P_{m_i} - P_i\right), \omega_i(0) = \omega_{i0}, \tag{1b}$$

$$\dot{E}'_{q_i} = \frac{1}{T'_{d_{0_i}}}\left(E_{f_i} - E_{q_i}\right), E'_{q_i}(0) = E'_{q_{i0}} \quad i = 1, \ldots, N, \tag{1c}$$

where

$$E_{q_i} = E'_{q_i} + \left(x_{d_i} - x'_{d_i}\right)I_{d_i},\ P_i = E'_{q_i}I_{q_i},\ Q_{e_i} = E'_{q_i}I_{d_i}, \tag{1d}$$

$$V_i = \sqrt{\left(x_{q_i}I_{q_i}\right)^2 + \left(E'_{q_i} - x_{d_i}I_{d_i}\right)^2}, \tag{1e}$$

and the direct I_{d_i} and quadratic I_{q_i} axis currents considering lossy transmission lines are given by

$$I_{q_i} = E'_{q_i}G_{ii} + \sum_{j\neq i}^{N} E'_{q_j}\left\{G_{ij}\cos\left(\delta_i - \delta_j\right) + B_{ij}\sin\left(\delta_i - \delta_j\right)\right\}, \tag{1f}$$

$$I_{d_i} = -E'_{q_i}B_{ii} + \sum_{j\neq i}^{N} E'_{q_j}\left\{G_{ij}\sin\left(\delta_i - \delta_j\right) + B_{ij}\cos\left(\delta_i - \delta_j\right)\right\}, \tag{1g}$$

where δ_i is the load angle, ω_i is the relative speed, P_i is the electrical power, P_{m_i} is the mechanical input power which is considered known, E_{f_i} is the voltage field, x_{q_i} is the quadrature axis reactance, x_{d_i} and x'_{d_i} are the direct and transient axis reactances, respectively, D_i is the per unit damping factor, H_i is the inertia constant, $T'_{d_{0_i}}$ is the direct axis transient short circuit time constant, respectively, Q_{e_i} is the reactive power, E_{q_i}' is the transient electromotive force in the quadrature axis, B_{ij} and G_{ij} are, respectively, the susceptance and conductance of the generator "i", V_i is the terminal voltage magnitude, and N is the number of generators connected to the grid.

In order to adopt the electrical power injected by generators into the grid as a state variable, the time derivative of P_i with respect to time is obtained as follows:

$$\dot{P}_i = \frac{1}{T_{d_{0_i}}'} E_{f_i} I_{q_i} - \frac{1}{T_{d_{0_i}}'} E_{q_i}' I_{q_i} - \frac{\left(x_{d_i} - x_{d_i}'\right)}{T_{d_{0_i}}'} I_{q_i} I_{d_i} + E_{q_i}' \dot{I}_{q_i}, \quad (2a)$$

where

$$\begin{aligned} \dot{I}_{q_i} = {} & \dot{E}_{q_i}' G_{ii} + \sum_{j \neq i}^{N} \dot{E}_{q_j}' \left\{ G_{ij} \cos\left(\delta_i - \delta_j\right) + B_{ij} \sin\left(\delta_i - \delta_j\right) \right\} - \sum_{j \neq i}^{N} E_{q_j}' \left\{ G_{ij} \sin\left(\delta_i - \delta_j\right) - B_{ij} \cos\left(\delta_i - \delta_j\right) \right\} \omega_i, \\ & - \sum_{j \neq i}^{N} E_{q_j}' \left\{ G_{ij} \sin\left(\delta_i - \delta_j\right) + B_{ij} \cos\left(\delta_i - \delta_j\right) \right\} \omega_j. \end{aligned} \quad (2b)$$

Thus, from (1a), (1b), and (2a), the large-scale MPS dynamic model can be represented by a variation of the standard three-dimensional flux decay model as follows:

$$\dot{\delta}_i = \omega_i, \delta_i(0) = \delta_{i0}, y_i = \delta_i \text{ or } \omega_i, \quad i = 1, \ldots, N, \quad (3a)$$

$$\dot{\omega}_i = -a_i \omega_i - b_i P_i + d_{\omega_i}, \omega_i(0) = \omega_{i0}, \quad (3b)$$

$$\dot{P}_i = -c_i P_i + \gamma_i\left(\boldsymbol{\delta}, \boldsymbol{\omega}, \mathbf{d}_\gamma, \mathbf{p}_i, \mathbf{p}_{I_i}\right) + u_i, \ P_i(0) = P_{i0}, \quad (3c)$$

where

$$\begin{aligned} \gamma_i\left(\boldsymbol{\delta}, \boldsymbol{\omega}, \mathbf{d}_\gamma, \mathbf{p}_i, \mathbf{p}_{I_i}\right) &= -c_i\left(x_{d_i} - x_{d_i}'\right)\left(I_{q_i} I_{d_i}\right) + E_{q_i}' \dot{I}_{q_i}, \\ \boldsymbol{\delta} &= \left[\delta_1, \ldots, \delta_N\right]^\top, \\ \boldsymbol{\omega} &= \left[\omega_1, \ldots, \omega_N\right]^\top, \\ d_{\omega_i} &= \left(\frac{1}{2H_i}\right) P_{m_i}, \\ \delta_i &\in A = [0, 2\pi], \\ \omega_i &\in \Omega_i = \left[0, \omega_i^+\right], \\ u_i &\in U_i = \left[u_i^-, u_i^+\right], \\ a_i &= \frac{D_i}{2H_i}, \\ b_i &= \frac{1}{2H_i}, \\ c_i &= \frac{1}{T_{d_{0_i}}'}, \\ \mathbf{p}_i &= \left[a_i, b_i, c_i, x_{d_i}, x_{d_i}'\right]^\top, \\ \mathbf{p}_{I_i} &= G_{ij} + B_{ij}, \\ \mathbf{w} &= \left[I_{d_i}, E_{q_i}', E_{q_j}', \dot{E}_{q_i}', \dot{E}_{q_j}', \omega_j\right]^\top, \\ \boldsymbol{\eta}_i &= \left[d_{w_i}, I_{q_i}\right]^\top, \\ \mathbf{d}_\gamma &= \left[\mathbf{w}, \boldsymbol{\eta}_i\right]^\top, \\ u_i &= c_i I_{q_i} E_{f_i}. \end{aligned} \quad (3d)$$

η_i and $\mathbf{w}$ are the measured vector and unmeasured vector input, respectively, y_i is the measured output, u_i is the control input associated with E_{fi}, γ_i is a (Lipschitz-bounded) nonlinear function, $\mathbf{p}_i$ and $\mathbf{p}_{I_i}$ are the local and interaction parameters, respectively.

In per-machine vector notation, the MPS NL model (3a)–(3d) is written as

$$\dot{\mathbf{x}}_i = \mathscr{A}_i \mathbf{x}_i + \mathbf{b}_d d_{\omega_i} + \mathbf{b}_u \left[\gamma_i\left(\mathbf{x}, \mathbf{d}_\gamma\right) + u_i\right], \mathbf{x}_i(0) = \mathbf{x}_{i_0}, \quad (4a)$$

$$\begin{aligned} y_i &= \mathbf{c}_y \mathbf{x}_i, \\ i &= 1, \ldots, \mathrm{N}, \end{aligned} \quad (4b)$$

where

$$\begin{aligned} \mathbf{x}_i &= \begin{bmatrix} \delta_i \\ \omega_i \\ P_i \end{bmatrix}, \\ \mathscr{A}_i &= \begin{bmatrix} 0 & 1 & 0 \\ 0 & -a_i & -b_i \\ 0 & 0 & -c_i \end{bmatrix}, \\ \mathbf{b}_u &= \begin{bmatrix} 0 \\ 0 \\ 1 \end{bmatrix}, \\ \mathbf{b}_d &= \begin{bmatrix} 0 \\ 1 \\ 0 \end{bmatrix}, \\ \mathbf{c}_y &= [1, 0, 0] \text{or} [0, 1, 0], \end{aligned} \quad (5)$$

$\gamma_i(\mathbf{x}, \mathbf{d}_{\gamma_i})$ is a Lipschitz-bounded function that englobes information about parameters, known and unknown inputs, nonlinearities, transmission losses, and intermachine interaction.

In compact form, the MPS NL model (4a) and (4b) is rewritten as

$$\dot{\mathbf{x}}_i = \mathbf{f}_i\left(\mathbf{x}_i, \mathbf{d}_{x_i}\right),$$
$$\mathbf{x}_i(0) = \mathbf{x}_{0_i}, \tag{5a}$$
$$y_i = \mathbf{c}_y\mathbf{x}_i, \quad \mathbf{x}_{0_i} \in X_{0_i} \subseteq X_i,\ \mathbf{x}_i \in X_i,\ \mathbf{d}_{x_i} \in D_{x_i},$$

where

$$\mathbf{f}_i\left(\overline{\mathbf{x}}_i, \overline{\mathbf{d}}_{x_i}\right) = \mathscr{A}_i\mathbf{x}_i + \mathbf{b}_d d_{\boldsymbol{\omega}_i} + \mathbf{b}_u\left[u_i + \gamma_i\left(\mathbf{x}, \mathbf{d}_{\gamma_i}\right)\right] = 0, \tag{5b}$$

$$\left\|\gamma_i\left(\mathbf{x}_i, \mathbf{d}_{\gamma_i}\right) - \gamma_i\left(\overline{\mathbf{x}}_i, \overline{\mathbf{d}}_{\gamma_i}\right)\right\| \le l_{\mathbf{x}}^{\gamma}\left\|\mathbf{x}_i - \overline{\mathbf{x}}_i\right\| + l_{\mathbf{d}_\gamma}^{\gamma}\left\|\mathbf{d}_{\gamma_i} - \overline{\mathbf{d}}_{\gamma_i}\right\|, \tag{5c}$$

where $\overline{\mathbf{x}}_i$ is a uniquely robust unstable nominal steady-state (SS) associated with the nominal input $\overline{\mathbf{d}}_{x_i}$, and γ_i is a Lipschitz-bounded function (5c) about the nominal operation.

Remark 1. In comparison with our previous work [27] as a practical modification (to be more realistic) for estimation purposes, the medium-length transmission line model is adopted whose single-phase equivalent model can be represented by π configuration. However, this assumption does not modify the conceptual idea behind the proposed estimation methodology. Also, a general study of transmission line losses can be done through the power nodal balances.

2.2. Estimation Objective. Based on the measurement of load angle and relative speed of generators, the problem consists in proposing a state estimation comprehensive design methodology for MPS that allows the independent estimation of dynamic state variables of generators $(\delta_i, \omega_i, P_i)$ along with terminal voltage magnitudes (V_i) with the following features: (i) a robustly convergent, computationally efficient, and linearly-decentralized dynamic state estimator, (ii) systematic construction based on a linearly-decentralized realization of the nonlinear representation of MPS (3), (iii) identification of the underlying observability condition based on two candidates' measured outputs, (iv) a priori (before simulation or testing) assurance of robust estimator functioning, and (iv) a simple conventional-type two-parameter per-machine gain tuning scheme with a transparent connection between gain choices and state estimate convergence features.

3. State Estimation Methodology

This section follows the methods of [27]; briefly, the proposed dynamic state estimation methodology for MPSs includes the following: (i) derivation of the augmented L-D model for estimation, (ii) the conceptual estimation problem, (iii) robust observability assessment based on two candidates output functions, i.e., the load angle and relative speed of each generator, (iv) construction of the convergent estimator based on the load angle measurement, (v) development of the convergent estimator based on the relative speed measurement, (vi) tuning scheme, and (vii) comparison with other observer-based approaches.

3.1. Estimation Model. The MPS (4a)-(4b) in per-machine ι_i -parametric form is expressed as:

$$\dot{\mathbf{x}}_i = \mathbf{A}_i\mathbf{x}_i + \mathbf{b}_d d_{\omega_i} + \mathbf{b}_u\left(u_i + \iota_i\right),$$
$$x_i(0) = x_{i0}, \tag{6a}$$

$$y_i = \mathbf{c}_y\mathbf{x}_i,$$
$$\iota_i = \gamma_i\left(\mathbf{x}, \mathbf{d}_\gamma\right), \quad i = 1, \ldots, \mathrm{N}, \tag{6b}$$

where

$$A_i = \begin{bmatrix} 0 & 1 & 0 \\ 0 & -a_i & -b_i \\ 0 & 0 & -c_i \end{bmatrix},$$
$$\left|e^{A_i t}\right| \le a_i e^{-\lambda_i t},$$
$$\lambda_i = \zeta_i^m w_i^m, \tag{7}$$
$$\lambda_i = \min\left(\zeta_i^m \varpi_i^m, \varpi_i^e\right)$$
$$\approx \begin{cases} \lambda_{1,2}^i = -\zeta_i^m \varpi_i^m \pm \left[\varpi_i^m \sqrt{1 - \zeta_i^{m2}}\right] j, \\ \lambda_3^i = -\varpi_i^e, \end{cases}$$

and $\lambda_{1,2}^i$ and λ_3^i are the three eigenvalues of $\mathbf{A}_i$ (6a), which can be uniquely solved in terms of i-th machine parameters as follows:

$$\left(\zeta_i^m, \varpi_i^m, \varpi_i^e\right) = \mathscr{F}\left(a_i, b_i, c_i\right). \tag{8}$$

Remark 2. L-D estimation model. To derive a decentralized linear model with unknown-reconstructible input, the expression $\gamma_i(\mathbf{x}, \mathbf{d}_\gamma)$ (3d) is defined as a new state variable ι_i which represents all the uncertainties, external disturbances, interaction among generator units, and known and unknown nonlinearities. This new variable ι_i differs concerning our previous approach [27] in the following: (i) the new one considers the effect of the losses in the transmission lines on generator dynamics, (ii) the old one was represented by the high order nonlinear terms obtained from the expansion in Taylor series (TS) about the nominal state-input pair $(\overline{\mathbf{x}}, \overline{\mathbf{d}}_\gamma)$ of $\gamma_i(\mathbf{x}, \mathbf{d}_\gamma)$ (corresponding to a purely inductive network), and (iii) the linear terms resulted from the TS expansion were included in the formulation of the matrix $\mathbf{A}_i$ for tuning purposes.

By assuming that the signal ι_i is in a slow-varying regime (SVR) concerning the exponential convergence speed ϖ_i^o of the observer (to be designed), the linear decentralized (L-D) estimation model has the following structure:

$$\dot{\mathbf{x}}_i = \mathbf{A}_i\mathbf{x}_i + \mathbf{b}_d d_{\omega_i} + \mathbf{b}_u\left(u_i + \iota_i\right),$$
$$\mathbf{x}_i(0) = \mathbf{x}_{i0}, \tag{8a}$$
$$y_i = \mathbf{c}_y\mathbf{x}_i$$

$$\dot{\iota}_i \approx 0,$$
$$\iota_i(0) = \iota_{i0}, \tag{8b}$$
$$i = 1, \ldots, \mathrm{N},$$

where ι_i is an unknown exogenous input signal.

In compact notation, the augmented linear decentralized (L-D) system (8a) and (8b) is written as

$$\dot{\chi}_i = \mathscr{A}_a\chi_i + \beta_d d_{\omega_i} + \beta_u u_i, \quad y_i = \kappa_{\delta,\omega}\chi_i, \quad i = 1, \ldots, N, \tag{9}$$

where

$$\chi_i = [\mathbf{x}_i, \iota_i]^\top, \quad \mathscr{A}_a = \begin{bmatrix} 0 & 1 & 0 & 0 \\ 0 & -a_i & -b_i & 0 \\ 0 & 0 & -c_i & 1 \\ 0 & 0 & 0 & 0 \end{bmatrix}, \quad \beta_d = \begin{bmatrix} \mathbf{b}_d \\ 0 \end{bmatrix}, \quad \beta_u = \begin{bmatrix} \mathbf{b}_u \\ 0 \end{bmatrix}, \quad \dim(\chi_i) = 4. \tag{10}$$

In our particular case, for estimator design purposes, the output function vector can be given by the following two candidates functions:

$$\kappa_\delta = [1, 0, 0, 0], \quad \kappa_\omega = [0, 1, 0, 0]. \tag{11}$$

The estimation model (the multimachine third-order model augmented with robustly quick observable states, one per machine) is a decentralized one (9). On the other hand, the current multimachine power system model is interconnected (3a)–(3d). The novelty of the proposed estimation approach resides in this fundamental difference between the actual plant and estimator models.

3.2. Estimation Problem. Driven by the measured input-output pair signals $(y_i, \mathbf{d}_i)(t)$ of the actual MPS (4a) and (4b), the dynamic data processor (dynamic state estimator) must produce a robustly convergent state estimates $\hat{\chi}_i(t)$, i.e.,

$$\hat{\chi}_{i_0} \approx \chi_{i0} \Rightarrow \hat{\chi}_i(t) \longrightarrow {}_r\chi_i(t) = \tau_i\left[t, \chi_{i_0}, \mathbf{d}_i(\cdot), y_i(t)\right] \in X, \quad y_i = \kappa_{\delta,\omega}\chi_i(t), \tag{12}$$

with

$$\chi_i = [\mathbf{x}_i, \iota_i]^\top, \quad \kappa_\delta = [1, 0, 0, 0], \quad \kappa_\omega = [0, 1, 0, 0], \quad \mathbf{d}_i = \left[d_{\omega_i}, u_i\right]^\top, \quad \dim(\hat{\chi}_i) = 4, \tag{13}$$

where χ_i is the augmented state variable vector considering the dynamic variables of each generator $\mathbf{x}_i$ (load angle, relative speed, and electrical power) along with the new state variable ι_i (one per machine), which is a robustly quick observable state that retains the information of interaction among generators, all the uncertainties, external disturbances, and known and unknown nonlinearities of the MPS system, $\mathbf{d}_i(\cdot)$ is the measured input vector, and y_i is the output function which can either be the load angle or relative speed of each generator.

Now, the main problem relies on robustly and instantaneously estimating for every time instant t the augmented state $\chi_i(t)$ (9) on the basis of the corresponding output vector (load angle or relative speed of generators), the known inputs $\mathbf{d}_i(\cdot)$ signals, and their time derivatives.

3.3. Robust Observability Assessment Based on Two Candidates Output Functions. The following subsections derive the observability conditions based on load angle and relative speed as output functions.

3.3.1. Load Angle Measurement. For this, firstly, based on the load angle measurement $(y_i = \delta_i)$, the observability matrix of the state-augmented estimation model (9) is obtained as follows:

$$\mathbf{O}_{\delta_i} = \begin{bmatrix} \kappa_\delta \\ \kappa_\delta\mathscr{A}_a \\ \kappa_\delta\mathscr{A}_a^2 \\ \kappa_\delta\mathscr{A}_a^3 \end{bmatrix} = \begin{bmatrix} 1 & 0 & 0 & 0 \\ 0 & 1 & 0 & 0 \\ 0 & -a_i & -b_i & 0 \\ 0 & a_i^2 & b_i(a_i + c_i) & -b_i \end{bmatrix}, \tag{14}$$

$$\det(\mathbf{O}_{\delta_i}) \neq_r 0 \Leftrightarrow b_i = \frac{D_i}{M_i} \neq_r 0, \quad i = 1, \ldots N. \tag{15}$$

The matrix pair $(\mathscr{A}_a, \kappa_\delta)$ of (9) is robustly observable because the coefficient b_i, associated with the inertia constant (M_i) of the i-th machine, is robustly strictly positive $b_i >_r 0$.

Remark 3. Observability Property. The observability condition (15) is the same as the one obtained in [27]; (14) shows almost no variations with respect to the preceding work [27] due to the differences involved in the construction of the L-D estimation model (9) as mentioned in Remark 2.

3.3.2. Relative Speed Measurement. A similar observability analysis is carried out under relative speed configuration as measured output function $(y_i = \omega_i)$. For this, as in the previous subsection, the L-D estimation model (9) is employed to obtain the observability matrix,

$$\mathbf{O}_{\omega_i} = \begin{bmatrix} \kappa_\omega \\ \kappa_\omega\mathscr{A}_a \\ \kappa_\omega\mathscr{A}_a^2 \end{bmatrix} = \begin{bmatrix} 1 & 0 & 0 \\ -a_i & -b_i & 0 \\ a_i^2 & b_i(a_i + c_i) & -b_i \end{bmatrix}, \tag{16}$$

$$\operatorname{rank}(\mathbf{O}_{\omega_i}) = 3, \quad \det(\mathbf{O}_{\omega_i}) \neq_r 0 \Leftrightarrow b_i = \frac{D_i}{M_i} \neq_r 0, \ i = 1, \ldots N. \tag{17}$$

The successive time derivations of the output map of the estimation model (9) draw three algebraic equation sets [38].

$$\begin{aligned}\psi_{\omega_i}(t) &= \mathbf{O}_{\omega_i}\boldsymbol{\chi}_{\omega_i} + \boldsymbol{\varrho}_{\omega_i}(t),\\ \boldsymbol{\chi}_{\omega_i} &= \left[\omega_i, P_i, \iota_i\right]^{\top}, \quad i = 1,\ldots \mathrm{N},\end{aligned} \tag{17a}$$

where

$$\begin{aligned}\boldsymbol{\psi}_{\omega_i}(t) &= \begin{bmatrix} y_i \\ \dot{y}_i \\ \ddot{y}_i \end{bmatrix},\\ \boldsymbol{\varrho}_{\omega_i}(t) &= \mathbf{T}_{\omega_i}\boldsymbol{\upsilon}_i,\\ \mathbf{T}_{\omega_i} &= \begin{bmatrix} 0 & 0 & 0 \\ 0 & \boldsymbol{\kappa}_{\omega}\boldsymbol{\beta}_d & 0 \\ \boldsymbol{\kappa}_{\omega}\mathscr{A}_a\boldsymbol{\beta}_u & \boldsymbol{\kappa}_{\omega}\mathscr{A}_a\boldsymbol{\beta}_d & \boldsymbol{\kappa}_{\omega}\boldsymbol{\beta}_d \end{bmatrix},\\ \boldsymbol{\upsilon}_i &= \left[u_i, d_{\omega_i}, \dot{d}_{\omega_i}\right]^{\top}.\end{aligned} \tag{17b}$$

The observability condition (17) establishes that the state of (9) is in the one-dimensional time-varying surface, as shown as follows:

$$\begin{aligned}X_{\delta_i}(t) &= \left\{\boldsymbol{\chi}_i \in X \mid \boldsymbol{\psi}_{\omega_i}(t) = \mathbf{O}_{\omega_i}\boldsymbol{\chi}_{\omega_i} + \boldsymbol{\varrho}_{\omega_i}(t)\right\},\\ \dim\left(X_{\delta_i}\right) &= 1.\end{aligned} \tag{18}$$

Accordingly, the restricted one-dimensional system is

$$\delta_i^*(t) = \tau_{x_i}^*\left[t, \delta_{i_0}, \boldsymbol{\psi}_{\omega_i}(t), \boldsymbol{\varrho}_{\omega_i}(t)\right] \in X_{\delta_i}(t), \tag{18a}$$

$$\begin{aligned}\dot{\delta}_i^*(t) &= \omega_i(t),\\ \delta_i^*(0) &= \delta_{i_0}^*, \quad i = 1,\ldots \mathrm{N},\end{aligned} \tag{18b}$$

where (18b) and (18a) are defined as the unobservable dynamics and motion, respectively.

Proposition 1. *If the unobservable motion $\delta_i^*(t)$ (18a) is exponentially (E)-stable, $(\delta_i^*, \psi_{\omega_i}, \boldsymbol{\varrho}_{\omega_i})$ produce an online reconstruction of $\chi_i(t)$ based on relative speed measurement $(y_i = \omega_i(t))$, the known inputs $(\mathbf{d}_i = [d_{\omega_i}, u_i]^{\top})$, and their time derivatives (up to adequate order) [28, 29].*

The plant and its unobservable motions coincide [i.e., $\delta_i^*(t) = \chi_i(t)$], but the same is not necessarily true for their stability properties. If $\chi_i(t)$ is stable, $\delta_i^*(t)$ is stable. If $\chi_i(t)$ is unstable, $\delta_i^*(t)$ can be stable or unstable [28, 29].

3.4. Estimator Design Based on Load Angle Measurement. The construction of the proposed L-D GE estimator based on load angle measurement for MPS (3a)–(3d) includes the effect of the losses in the transmission lines on generator dynamics and closely follows the estimation methodology reported in [27]. In this present study, only the main construction steps are presented. Moreover, a method focused on estimating the terminal voltage magnitudes from estimated state variables is proposed.

In summary, the robustly convergent observer in χ_i-coordinate is written as

$$\dot{\hat{\boldsymbol{\chi}}}_i = \mathbf{f}_i(\hat{\boldsymbol{\chi}}_i, \mathbf{d}_i) + \mathbf{k}_{\delta_i}^o(\zeta_i^o, \varpi_i^o)(y_i - \kappa_\delta\hat{\boldsymbol{\chi}}_i), \quad i = 1,\ldots,\mathrm{N}, \tag{19}$$

where

$$\mathbf{k}_{\delta_i}^o(\zeta_i^o, \varpi_i^o) = \left[\mathbf{O}_{\delta_i}^{-1}\right]\left[4\zeta_i^o\varpi_i^o, \left(4\zeta_i^{o2} + 2\right)\varpi_i^o, 4\zeta_i^o\varpi_i^{o3}, \varpi_i^{o4}\right]^{\top} = \left(k_i^\delta, k_i^\omega, k_i^P, k_i^\iota\right)^{\top}(\zeta_i^o, \varpi_i^o), \tag{19a}$$

$$\begin{aligned}k_i^\delta(\zeta_i^o, \varpi_i^o) &= 4\zeta_i^o\varpi_i^o,\\ k_i^\omega(\zeta_i^o, \varpi_i^o) &= \left(4\zeta_i^{o2} + 2\right)\varpi_i^{o2},\end{aligned} \tag{19b}$$

$$k_i^P(\zeta_i^o, \varpi_i^o) = -\left(\frac{a_i}{b_i}\right)\left(4\zeta_i^{o2} + 2\right)\varpi_i^{o2} - \left(\frac{1}{b_i}\right)4\zeta_i^o\varpi_i^{o3}, \tag{19c}$$

$$k_i^\iota(\zeta_i^o, \varpi_i^o) = \left(\frac{-c_i a_i}{b_i}\right)\left(4\zeta_i^{o2} + 2\right)\varpi_i^{o2} - \left(\frac{(c_i + a_i)}{b_i}\right)4\zeta_i^o\varpi_i^{o3} - \left(\frac{1}{b_i}\right)\varpi_i^{o4}. \tag{19d}$$

The vector gain in χ_i coordinates changed in comparison with the one derived in [27] on account that the observability matrix is different in both cases despite considering the same measured output (based on the load angle measurement). Mainly, the main difference relies on constructing the new L-D estimation model as mentioned in Remark 3.

The robustly convergent estimation error of the MPS estimator (19) is EU-bounded as shown as follows:

$$\left|\tilde{\chi}_i(t)\right| \le a_i^{\chi} e^{-\lambda_i^o t}\left|\tilde{\chi}_{i_0}\right| + \left(\frac{a_i^{\chi}}{\lambda_i^o}\right)\epsilon_{\theta_i}, \quad i = 1, \ldots \infty, \mathrm{N}. \tag{20}$$

The linear-decentralized observer in (x_i, ι_i) coordinates is given by

$$\begin{aligned}\dot{\hat{\mathbf{x}}}_i &= \mathbf{A}_i\hat{\mathbf{x}}_i + \mathbf{b}_d d_{\omega_i} + \mathbf{b}_u\left(u_i + \hat{\iota}_i\right) + \mathbf{k}_i^{\mathbf{x}}\left(\zeta_i^o, \varpi_i^o\right)\left(y_i - \mathbf{c}_y\hat{\mathbf{x}}_i\right),\\ \hat{\mathbf{x}}_i(0) &= \hat{\mathbf{x}}_{i_0},\end{aligned} \tag{20a}$$

$$\begin{aligned}\dot{\hat{\iota}}_i &= k_i^{\iota}\left(\zeta_i^o, \varpi_i^o\right)\left(y_i - \mathbf{c}_y\hat{\mathbf{x}}_i\right),\\ \hat{\iota}_i(0) &= \iota_{i_0}, \quad i = 1, \ldots, \mathrm{N},\end{aligned} \tag{20b}$$

where

$$\begin{aligned}\mathbf{k}_i^{\mathbf{x}}\left(\zeta_i^o, \varpi_i^o\right) &= \left(k_i^{\delta}, k_i^{\omega}, k_i^{P}\right)^{\top}\left(\zeta_i^o, \varpi_i^o\right),\\ k_i^{\iota} &= k_i^{\iota}\left(\zeta_i^o, \varpi_i^o\right).\end{aligned} \tag{21}$$

In detailed form, the L-D GE estimator (20a) and (20b) in open-loop configuration for the MPS is written as follows:

$$\dot{\hat{\delta}}_i = \hat{\omega}_i + k_i^{\delta}\left(\zeta_i^o, \varpi_i^o\right)\left(y_i - \hat{\delta}_i\right), \hat{\delta}_i(0) = \hat{\delta}_{i_0}, y_i = \delta_i, \tag{21a}$$

$$\dot{\hat{\omega}}_i = -a_i\hat{\omega}_i - b_i\hat{P}_i + d_{\omega_i} + k_i^{\omega}\left(\zeta_i^o, \varpi_i^o\right)\left(y_i - \hat{\delta}_i\right), \hat{\omega}_i(0) = \omega_{i_0}, \tag{21b}$$

$$\dot{\hat{P}}_i = -c_iP_i + \hat{\iota}_i + u_i + k_i^{P}\left(\zeta_i^o, \varpi_i^o\right)\left(y_i - \hat{\delta}_i\right), \hat{P}_i(0) = \hat{P}_{i_0}, \tag{21c}$$

$$\dot{\hat{\iota}}_i = k_i^{\iota}\left(\zeta_i^o, \varpi_i^o\right)\left(y_i - \hat{\delta}_i\right), \hat{\iota}_i(0) = \hat{\iota}_{i_0}, \quad i = 1, \ldots, \mathrm{N}. \tag{21d}$$

Then, the successfully estimated values of the augmented state $\chi_i(t)$ from the proposed L-D GE estimator (20a) and (20b) are involved in the estimation of terminal voltage magnitudes.

For this, given the estimation of $\hat{P}_i$ and assuming that the known input $I_{q_i} \neq 0$ (it is valid for normal operationally conditions [39]), an estimated value of E_{q_i}' can be computed as

$$\hat{E}_{q_i}' = \frac{\hat{P}_i}{I_{q_i}}, \quad i = 1, \ldots, \mathrm{N}, \tag{22}$$

and

$$\hat{I}_{d_i} = -\hat{E}_{q_i}'B_{ii} + \sum_{j \neq i}^{\mathrm{N}} \hat{E}_{q_j}'\left\{G_{ij}\sin\left(\hat{\delta}_i - \hat{\delta}_j\right) + B_{ij}\cos\left(\hat{\delta}_i - \hat{\delta}_j\right)\right\}, \quad i = 1, \ldots, \mathrm{N}. \tag{23}$$

Then, we have

$$\hat{V}_i = \sqrt{\left(x_{q_i}I_{q_i}\right)^2 + \left(\hat{E}_{q_i}' - x_{d_i}\hat{I}_{d_i}\right)^2} \quad i = 1, \ldots, \mathrm{N}. \tag{24}$$

The proposed L-D GE estimator (20a) and (20b) allows estimating of dynamic state variables (load angle, relative speed, and electrical power) associated with the N generators together with the terminal voltage magnitudes by employing the load angle as the unique measured output along with local information (composed by the known input pair $\mathbf{d}_i = [d_{\omega_i}, u_i]^{\top}$, as well as I_{q_i} is assumed to be known).

3.5. Estimator Design Based on Relative Speed Measurement. If the unobservable motion $\delta_i^*(t)$ (18a) is robustly exponentially (RE)-stable (the stability of load angle of a third-order synchronous generator employed in MPS studies has been analyzed in [35, 40]; thus, the unobservable dynamics do not affect the stability of power systems), the online integration of the auxiliary estimator based on relative speed measurement is expressed as

$$\begin{aligned}\dot{\hat{\chi}}_i &= \mathbf{f}_i(\hat{\chi}_i, \mathbf{d}_i) + \mathbf{k}^o_{\omega_i}(\zeta^o_i, \varpi^o_i)(y_i - \kappa_\omega \hat{\chi}_i),\\ \hat{\chi}_i(0) &= \hat{\chi}_{i_0} \neq \chi_{i_0},\\ \hat{\chi}_i &\in X_{\delta_i}(t),\end{aligned} \tag{25}$$

where

$$\mathbf{k}^o_{\omega_i}(\zeta^o_i, \varpi^o_i) = \left[0, \left(\mathbf{O}_{\omega_i}\right)^{-1}\right]^\top \left[0, (2\zeta^o_i + 1)\varpi^o_i, (2\zeta^o_i + 1)\varpi^{o2}_i, \varpi^{o3}_i\right]^\top, \tag{26}$$

yields a motion $\hat{\chi}_i(t)$ that RE-converges to the plant motion $\chi_i(t)$ according to the inequality

$$\left|\hat{\chi}_i - \chi_i\right| \leq a^\chi_i e^{-\lambda^o_i t}\left|\tilde{\chi}_{i_0}\right| + \left(\frac{a^\chi_i}{\lambda^o_i}\right)\epsilon_{\theta_i}, \hat{\chi}_i, \chi_i \in X_{\delta_i}(t), \quad i = 1, \ldots, \mathrm{N}. \tag{27}$$

In $(\mathbf{x}_i, \iota_i)$-coordinates (25), the L-D GE estimator is written as

$$\begin{aligned}\dot{\hat{\delta}}_i &= \hat{\omega}_i,\\ \hat{\delta}_i(0) &= \hat{\delta}_{i_0},\end{aligned} \tag{28a}$$

$$\begin{aligned}\dot{\hat{\omega}}_i &= -a_i\hat{\omega}_i - b_i\hat{P}_i + d_{\omega_i} + g_{\omega_i}(\zeta^o_i, \varpi^o_i)(\omega_i - \hat{\omega}_i),\\ \hat{\omega}_i(0) &= \hat{\omega}_{i_0},\end{aligned} \tag{28b}$$

$$\begin{aligned}\dot{\hat{P}}_i &= -c_i\hat{P}_i + \hat{\iota}_i + u_i + g_{P_i}(\zeta^o_i, \varpi^o_i)(\omega_i - \hat{\omega}_i),\\ \hat{P}_i(0) &= \hat{P}_{i_0},\end{aligned} \tag{28c}$$

$$\begin{aligned}\dot{\hat{\iota}}_i &= g_{\iota_i}(\varpi^o_i)(\omega_i - \hat{\omega}_i),\\ \hat{\iota}_i(0) &= \hat{\iota}_{i_0},\end{aligned} \tag{28d}$$

where the output-driven corrector for the i-th subsystem is expressed as

$$\begin{bmatrix} g_{\omega_i}(\zeta^o_i, \varpi^o_i) \\ g_{P_i}(\zeta^o_i, \varpi^o_i) \\ g_{\iota_i}(\varpi^o_i) \end{bmatrix} = \begin{bmatrix} (2\zeta^o_i + 1)\varpi^o_i \\ -\dfrac{a_i}{b_i}(2\zeta^o_i)\varpi^o_i - \dfrac{1}{b_i}(2\zeta^o_i + 1)\varpi^{o2}_i \\ -\dfrac{a_i c_i}{b_i}(2\zeta^o_i + 1)\varpi^o_i - \dfrac{a_i + c_i}{b_i}(2\zeta^o_i + 1)\varpi^{o2}_i - \dfrac{1}{b_i}\varpi^{o3}_i \end{bmatrix}. \tag{29}$$

Also, the estimation of terminal voltage magnitudes is obtained utilizing estimated state variables from (28a)–(28d) through (24).

Remark 4. Robust Convergence. A similar analysis of the estimation error dynamics of the proposed L-D GE estimators (19) and (25) based on the current MPS model (considering unmodeled parasitic dynamics) can be carried out as the one presented in [27]. Thus, the estimation error dynamics will be robustly exponentially (RE)-stable if the observer frequencies ϖ_i^o, one per machine, are chosen so that the stabilizing terms (λ_{s_i}) dominate the potentially destabilizing ones (λ_{d_i}) [27, 28, 30].

3.6. Tuning Scheme. The tuning guideline is derived from the pole placement approach regarding damping-frequency pairs (ζ_i^o, ϖ_i^o). For the L-D GE estimator based on load angle measurement, the reference gain $\mathbf{k}_{\delta_i}^o$ (19a) of (19) relies closely on the proposed methodology in [28–30]. This one is based on its counterpart in z-coordinates (one per machine), according to the characteristic polynomials of the prescribed linear, noninteractive, pole assignable (*LNPA*) output error dynamics

$$[L_i(p_i, \varpi_i^o)]\tilde{y}_i := \tilde{y}_i^{(4)} + 4\zeta_i^o\varpi_i^o\tilde{y}_i^{(3)} + \left(4\zeta_i^{o2} + 2\right)\varpi_i^{o2}\tilde{y}_i^{(2)} + \left(4\zeta_i^o\varpi_i^{o3}\right)\tilde{y}_i^{(1)} + \varpi_i^{o4}\tilde{y}_i = 0, \tag{29a}$$

where

$$\begin{aligned}\tilde{y}_i &= \hat{y}_i - y_i,\\ \hat{y}_i &= \boldsymbol{\kappa}_\delta\hat{\mathbf{z}}_i, \quad i = 1, \ldots, \mathrm{N},\end{aligned} \tag{29b}$$

where the pole configuration (or frequency gain vector) can be set with a standard or tailored form (ITAE stands for integral of time-weight absolute error, Butterworth), [41], and L_i is the associated linear operator.

For the fourth-degree polynomial (29a) motivated by optimal linear-quadratic regulator (LQR) and nonlinear (NL) extended Kalman filter (EKF), as well as GE [28, 29], the prescribed pole pattern associated with (29a) is given by two complex-conjugate pole pairs with damping frequency pair as follows:

$$\begin{aligned}\nu_{1,2}^i &= -\zeta_i^o\varpi_i^o \pm \left[\varpi_i^o\sqrt{1 - \zeta_i^{o2}}\right]j,\\ \nu_{3,4}^i &= -\zeta_i^o\varpi_i^o \pm \left[\varpi_i^o\sqrt{1 - \zeta_i^{o2}}\right]j,\end{aligned} \tag{30}$$

where

$$\zeta_i^o = n_i^\zeta\zeta_i^m, n_i^\zeta = n_\zeta \in [1, 6] := \mathcal{J}_\zeta\varpi_i^o = n_i^\varpi\varpi_i^m, n_i^\varpi = n_\varpi \in [10, 50] := \mathcal{J}_\varpi, \tag{31}$$

Whereas for the L-D GE estimator based on relative speed measurement (28a)–(28d), the output-driven corrector $\kappa_{\omega_i}^o$ (26) is based on the prescribed vector gain associated with its counterpart in *z*-coordinates as well, which is defined according to the *LNPA* output error dynamics as

$$[L_i(p_i, \varpi_i^o)]\tilde{y}_i := \tilde{y}_i^{(3)} + (2\zeta_i^o + 1)\varpi_i^o\tilde{y}_i^{(2)} + (2\zeta_i^o + 1)\varpi_i^{o2}\tilde{y}_i^{(1)} + \varpi_i^{o3}\tilde{y}_i = 0, \tag{31a}$$

where

$$\begin{aligned}\tilde{y}_i &= \hat{y}_i - y_i,\\ \hat{y}_i &= \boldsymbol{\kappa}_\omega\hat{\mathbf{z}}_i, \quad i = 1, \ldots.\mathrm{N}.\end{aligned} \tag{31b}$$

The poles related to (31a) are assigned as a pair of complex-conjugate poles with reference characteristic frequency ϖ_i^o, and a sufficiently large ($\zeta_i^o > 0.71$) damping factor and one pole is set to be real with characteristic frequency ϖ_i^o, as shown as follows:

$$\begin{aligned}\nu_{1,2}^i &= -\zeta_i^o\varpi_i^o \pm \left[\varpi_i^o\sqrt{1 - \zeta_i^{o2}}\right]j,\\ \nu_3^i &= -\varpi_i^o,\end{aligned} \tag{32}$$

where

$$\begin{aligned}\zeta_i^o &= n_i^\zeta\zeta_i^m,\\ n_i^\zeta &= n_\zeta \in [1, 6] := \mathcal{J}_\zeta\varpi_i^o = n_i^\varpi\varpi_i^m,\\ n_i^\varpi &= n_\varpi \in [10, 50] := \mathcal{J}_\varpi.\end{aligned} \tag{33}$$

The proposed tuning scheme exploits the natural characteristics of MPS to obtain a better functioning in terms of an adequate compromise between speed reconstruction and tolerance to measurement noise with a conventional-like simple, transparent, and easy-to-apply tuning procedure based on two-parameter tuning.

3.7. Comparison with Other Observer-Based Approaches. In comparison with the conventional nonlinear-centralized (NL-C) EKF (based on the stochastic version of the MPS model by considering a global set of generators (3a)–(3d) in compact form) and nonlinear-decentralized (NL-D) SMPO [23] estimators for MPSs, the novelties are (i) from a theoretical perspective, the comprehensiveness of the methodology, and (ii) from an industrial applicability viewpoint; it is a more systematic and scalable design with a priory guarantee of reliable functioning and an admissible small online computational load (considerably smaller than the one of the NL-C EKF and similar to the one of the NL-D SMPO) and a substantially simpler easy-to-apply (preferably conventional-like) tuning scheme.

Concerning the NL-D SMPO estimator [23], the aims are as follows: (i) to retain its low-dimensionality and ability to reject modeling errors, (ii) to remove the fragility due to measurement noise propagation, and (iii) to simplify its rather complex tuning scheme. Concerning the conventional NL-C EKF estimator, the aims are as follows: (i) to retain its tolerance to measurement noise, (ii) to significantly reduce its online computational load, and (iii) to overcome the drawback of not having formal convergence proof.

4. Results and Discussion

The Western System Coordinating Council (WSCC) 9-bus electrical power grid is used [2, 4, 5, 7, 8, 36] to demonstrate the estimator's performance. The WSCC employed for evaluation purposes is shown in Figure 1, and the system's nominal parameters and the operations used for the sample problem investigated are listed in Table 1.

4.1. Tuning. The adjustable vectors $\mathbf{k}^o_{\delta_i}$ (19a) and $\mathbf{k}^o_{\omega_i}$ (26) are set according to the tuning procedure mentioned previously. For the L-D GE estimators (17) and (25), the damping-frequency tuning pair is set with: $\zeta^o_1 = 0.71$, $\zeta^o_{2,3} = 1.5$, $\varpi^o_1 = 60$, $\varpi^o_2 = 35$, and $\varpi^o_3 = 67$.

4.2. Testing Scheme. The measurements are affected by fluctuations driven by low-amplitude and high-frequency (close to resonant one) sinusoidal inputs, as shown as follows:

$$\begin{aligned} y_1 &= \delta_1 + 1e^{-4}\sin(600t),\\ y_2 &= \delta_2 + 1e^{-4}\sin(350t),\\ y_3 &= \delta_3 + 1e^{-4}\sin(670t). \end{aligned} \tag{34}$$

Moreover, the robust testing scheme considers different operation conditions as given as follows: (i) when generator one is affected by an unknown electromagnetic disturbance involving the excitation winding, which suddenly appears at $t = 1$ [sec], the fault is cleared after 0.5 seconds (clearing time t_{cl}); in this sense, the generator comes back to its prefault configuration, (ii) in parameter uncertainty, the value associated with the time constant $T_{d_1}{}'$ fluctuates around 15% and 25% from its original values through the time simulation, (iii) once the machines reach the steady-state regime, generator two is affected by a mechanical power variation at $t = 30$ [sec], which is cleared after 0.1 seconds, and (iv) to evaluate the transient performance of the L-D GE estimators, initial condition uncertainty has been considered for both estimation schemes (with respect to operation points).

The proposed robust testing scheme considers initial conditions errors, noisy measurements, and known/unknown disturbances. These testing conditions are more complex than those employed in previous estimation studies [7–10, 14, 23, 36].

Figures 2–7 depict the performance of estimators. Solid yellow lines represent the actual values of the load angle, relative speed, electrical power, and the nonlinear interconnection term of each machine; on the other hand, the dashed lines are used to show the estimated variables by both estimators of the L-D GE (19) in magenta and L-D GE (25) in cyan.

As can be appreciated, the transient behavior related to the abovementioned conditions is correctly reconstructed by both L-D GE estimators, which have a fast convergence rate to the actual states. Also, as can be noticed, the performance of the L-D GE (28a)–(28d) is similar to the one obtained through the L-D GE (20a) and (20b) based on the load angle measurement. The latter is lightly affected by measurement noise, as shown in Figures 3 and 5, specifically in estimating the nonlinear interconnection terms. The estimated signals from the L-D GE estimators can be used for monitoring purposes, particularly for designing observer-based controllers to enhance the transient stability of each generator in a decentralized fashion. As mentioned earlier, generator one is affected by an unknown exogenous input at $t = 1$ [sec]; the proposed estimators correctly estimate the dynamic state variables due to the fact that the unknown disturbance is included in the nonlinear interconnection term (ι_i), and it is reconstructed along with the other state variables.

Figure 8 shows the estimation of terminal voltage magnitudes, which are correctly reconstructed from the estimated state variables of each generator. However, the noise effect is notorious in the estimated variables by the L-D GE estimator on the basis of the load angle measurement (19). Therefore, we want to highlight that the disturbance which affects generator two at $t = 30$ [sec] is reflected in an extreme condition of MPS (for comparative academic purposes). Despite this, the transient and steady-state regimes are suitably captured by both L-D GE estimators.

Remark 5. Online Computational Load. The WSCC type 3-machine 9-bus system under the centralized extended Kalman filter approach (based on the stochastic version of the MPS model by considering a global set of generators

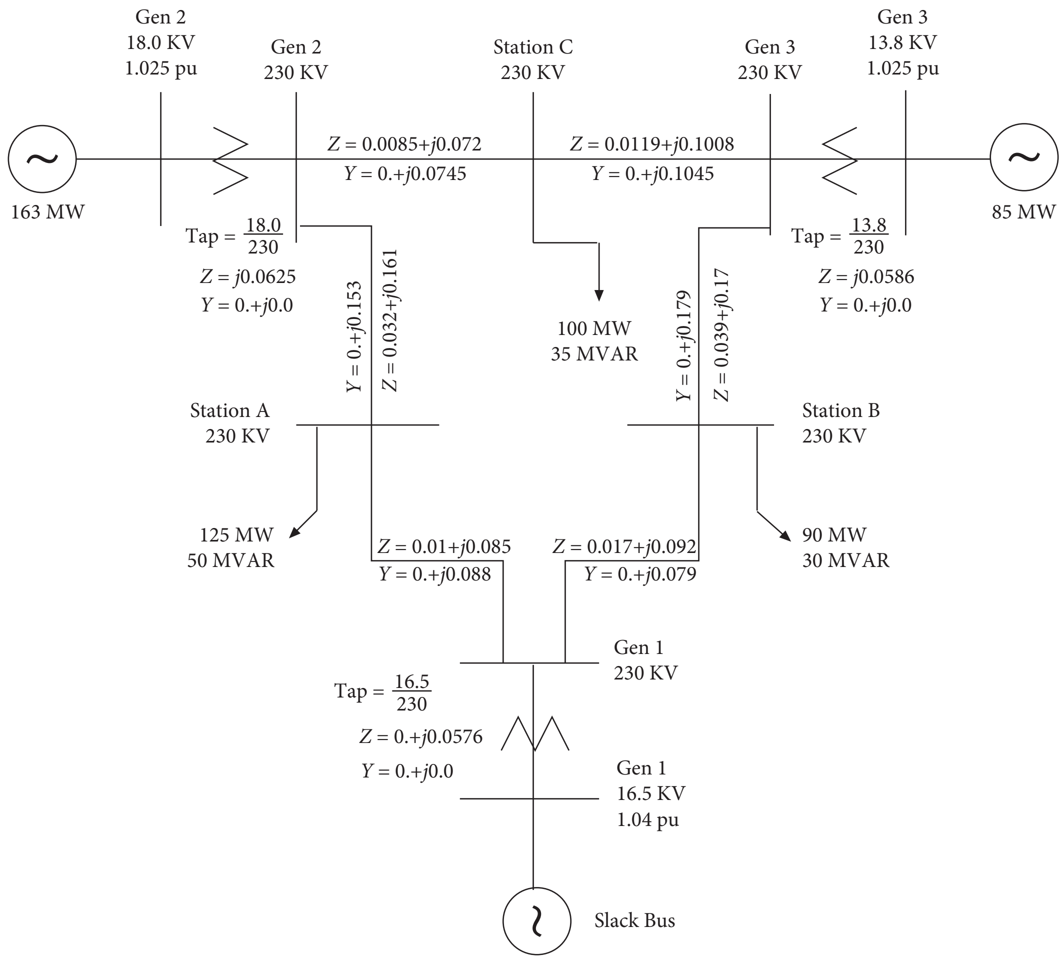

Figure 1: WSCC 3-machine, 9-bus system [2].

Table 1: Machine data.

Parameters	Generator 1	Generator 2	Generator 3
D_i (p.u.), $T'_{d_{0_i}}$ (s)	6, 8.96	5, 6	2, 5.89
H_i (s)	23.1	6.1	3.01
x'_{d_i} (p.u.), x_{d_i} (p.u.), x_{q_i} (p.u.)	0.0608, 0.146, 0.0969	0.1198, 0.8958, 0.8645	0.1813, 1.3125, 1.2578
E_{f_i} (p.u.)	1.056	1.789	1.403
P_{m_i} (p.u.)	0.716	1.63	0.85

(3a)–(3d) in compact form [27]) requires solving 54 ordinary differential equations (ODEs) due to the fact that the Riccati equations grow quadratically according to the number of state variables to be estimated. In the opposite case, the two proposed L-D GE estimators (19) and (25) only solve 12 ODEs (4 ODEs for each machine, considering the augmented state, which efficiently retains the interconnection information among machines). This difference can be made further significant in electrical power grids with many generators.

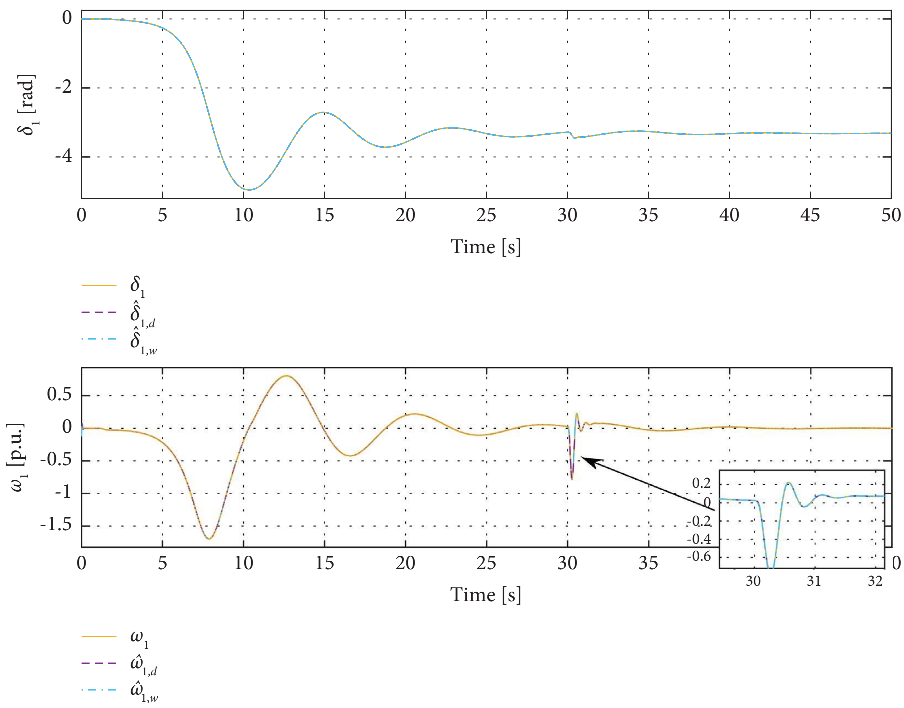

Figure 2: Comparison between the L-D GE estimators: load angle and relative speed of generator one.

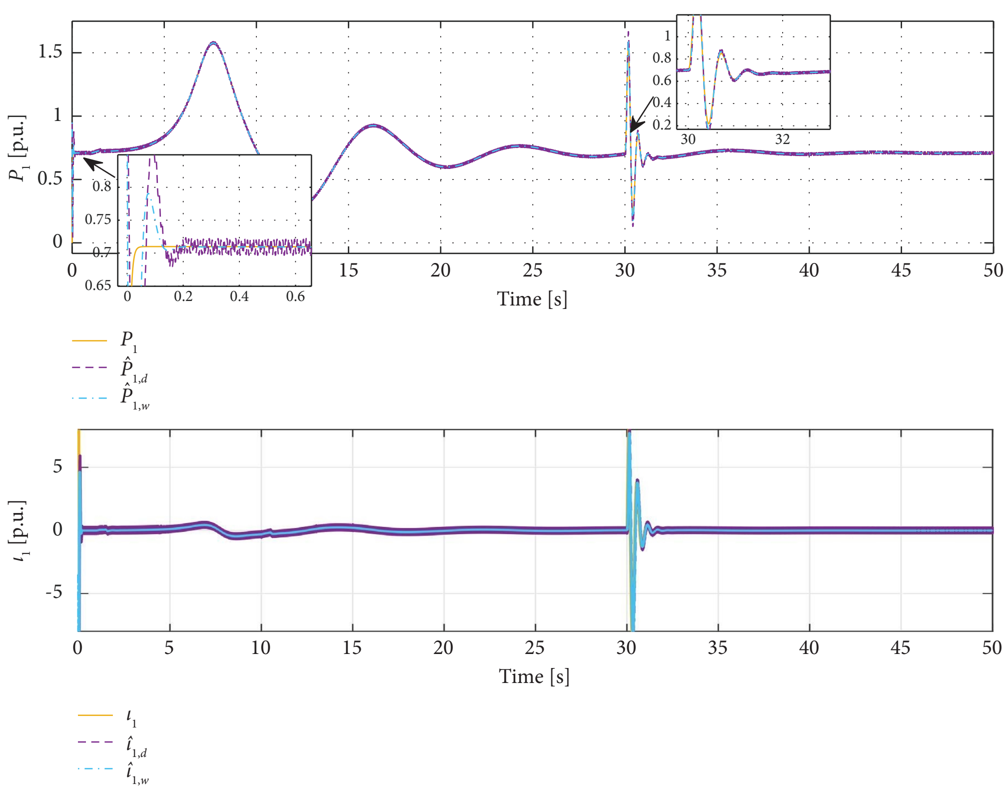

Figure 3: Comparison between the L-D GE estimators: the electrical power and nonlinear interconnection term of generator one.

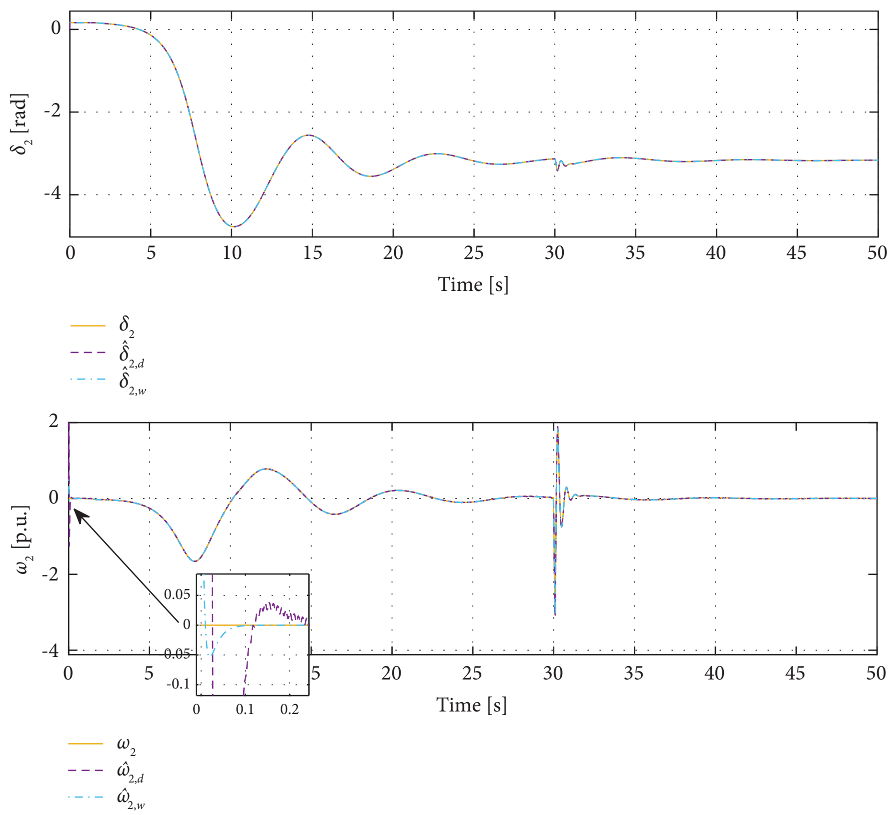

Figure 4: Comparison between the L-D GE estimators: load angle and relative speed of generator two.

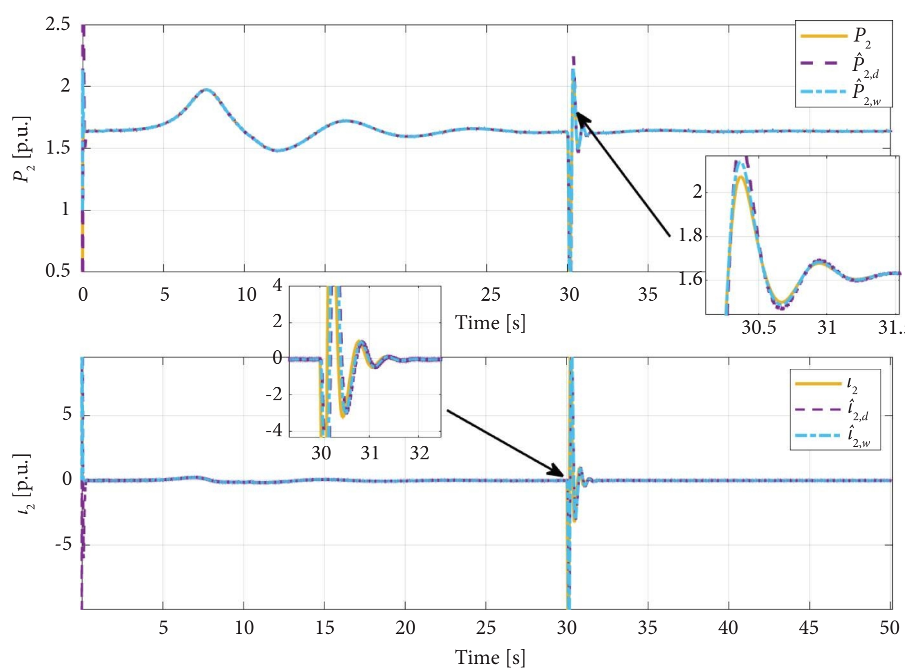

Figure 5: Comparison between the L-D GE estimators: the electrical power and nonlinear interconnection term of generator two.

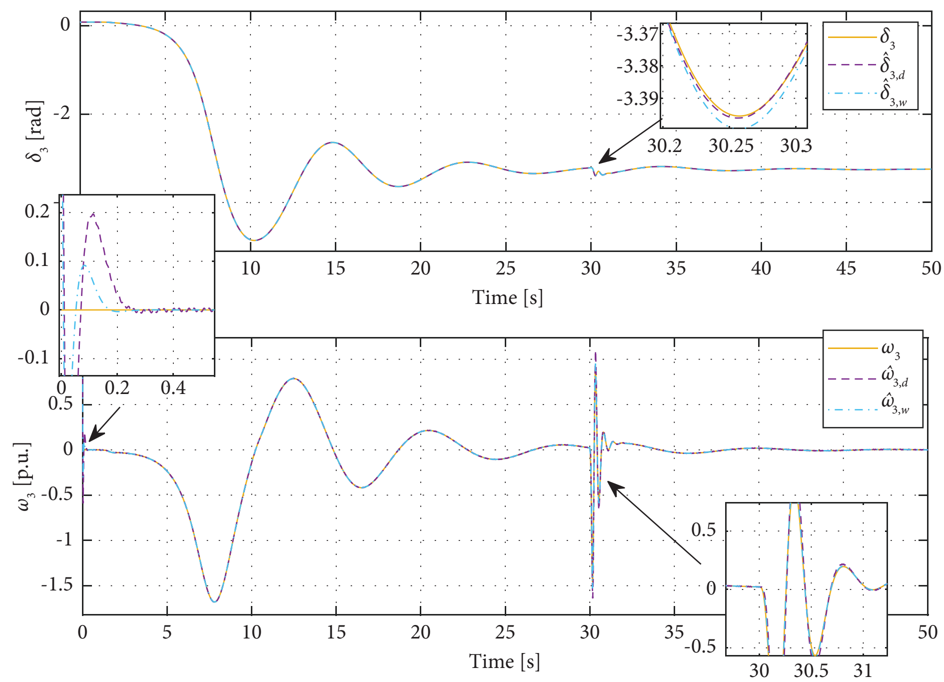

Figure 6: Comparison between the L-D GE estimators: load angle and relative speed of generator three.

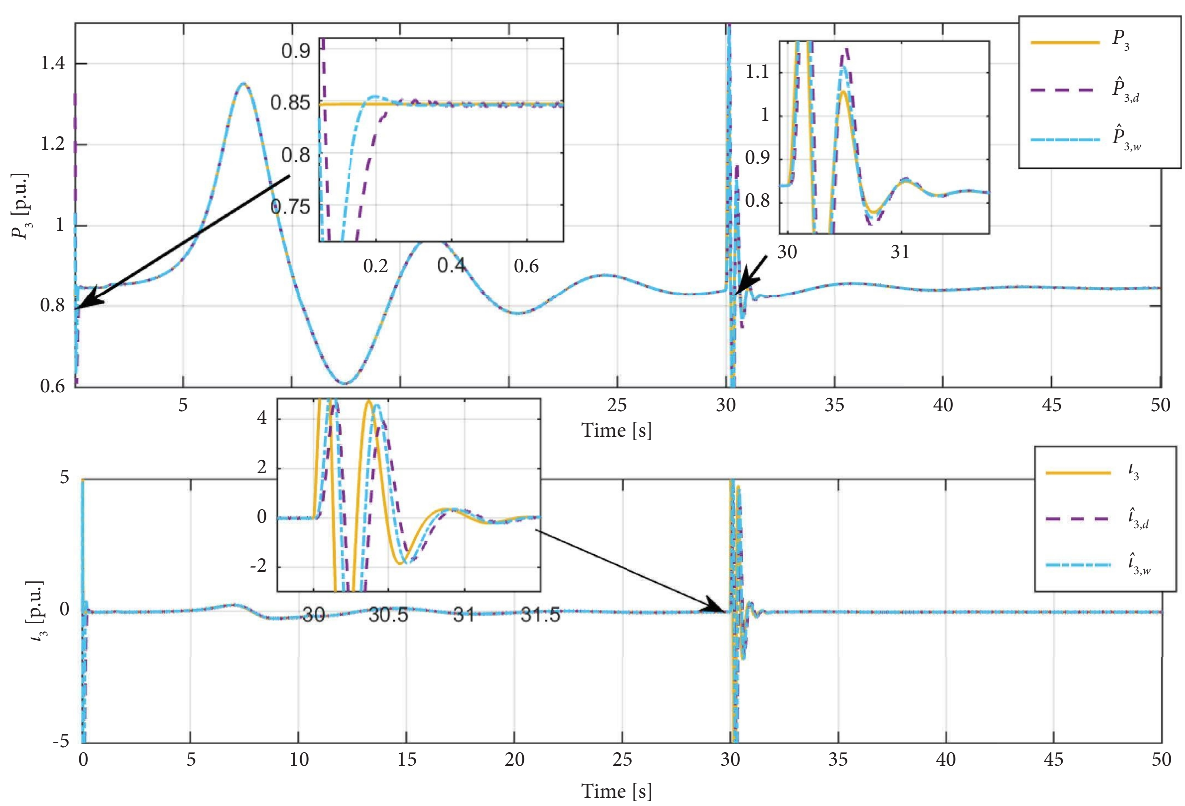

Figure 7: Comparison between the L-D GE estimators: the electrical power and nonlinear interconnection term of generator three.

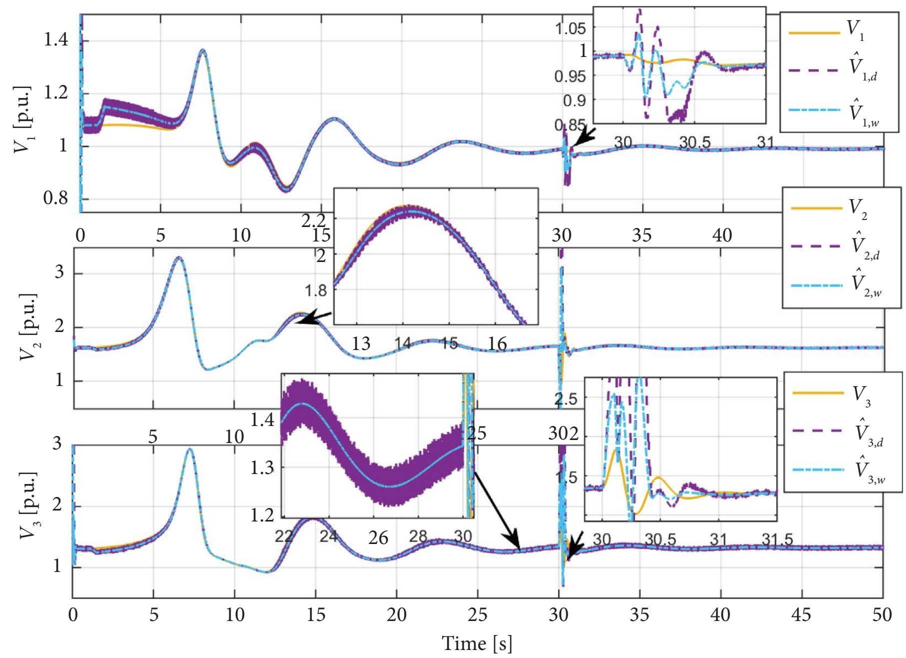

Figure 8: Estimation of voltage magnitudes through the proposed L-D GE estimators.

5. Conclusions

In this work, two robust linear decentralized (L-D) geometric estimators (GE) are proposed, one considering the load angle as measurement (19) and another one based on relative speed as measured output (25). Methodologically speaking, (i) both estimators are constructed based on a new representation of the classical flux decay MPS dynamic model by adopting the electrical power as a state variable to include the effect of the transmission losses on generators' dynamics, (ii) the new MPS dynamic model (3a)–(3d) is employed to construct an L-D estimation model (9), for which the state variables of generators are augmented by considering a set of new state variables (one per machine), these new variables stand for all the uncertainties, external disturbances, interaction among generator units, and known and unknown nonlinearities, (iii) the observability properties of the L-D estimation model (9) were identified for each measured output, for load angle (15) and the relative speed (17), respectively, (iv) both estimators have a precise and systematic industrial-like tuning based on two parameters associated with the generators' dynamics, (v) the proposed L-D state estimation schemes are computationally efficient (the involved ODEs by the estimators grow linearly for states to be estimated, almost a quarter of the total ODEs of the conventional EKF [27]), and (vi) both estimators have a robust convergence based on input-to-state (IS) stability and small gain ideas (as one presented in [27]).

The performance of the L-D GE estimators was evaluated via numerical simulations through a robust testing scheme considering known/unknown disturbances and noisy measurements. As a result, the developed dynamic estimators show a fast convergence rate to the current states of MPS and robust performance against measurement noises and initial condition uncertainties.

The present study on MPS estimation is a point of departure to address the observer-based output-feedback control design problem with an application-oriented robust decentralized scheme.

Data Availability

The used or generated data and the result of this study can be obtained from the corresponding author upon request.

Conflicts of Interest

The authors declare that they have no conflicts of interest regarding the publication of this paper.

Acknowledgments

This work was supported by Becas Posdoctorales DGAPA, UNAM.

References

[1] P. Kundur, N. J. Balu, and M. G. Lauby, *Power system stability and control*, McGraw-Hill, New York, NY, USA, vol. 7, 1994.

[2] P. W. Sauer and M. A. Pai, *Power system dynamics and stability*, Prentice hall Upper, Saddle River, NJ, USA, vol. 101, 1998.

[3] Y. Wang, G. Guo, and D. J. Hill, "Robust decentralized nonlinear controller design for multimachine power systems," *Automatica*, vol. 33, no. 9, pp. 1725–1733, 1997.

[4] X. Liu and Y. Han, "Decentralized multi-machine power system excitation control using continuous higher-order sliding mode technique," *International Journal of Electrical Power & Energy Systems*, vol. 82, pp. 76–86, 2016.

[5] A. Colbia-Vega, J. de Leon-Morales, L. Fridman, O. Salas-Pena, and M. Mata-Jiménez, "Robust excitation control design using sliding-mode technique for multimachine power

systems," *Electric Power Systems Research*, vol. 78, no. 9, pp. 1627–1634, 2008.

[6] T. K. Roy, M. A. Mahmud, and A. M. T. Oo, "Robust adaptive backstepping excitation controller design for higher-order models of synchronous generators in multimachine power systems," *IEEE Transactions on Power Systems*, vol. 34, no. 1, pp. 40–51, 2019.

[7] Z. Huang, K. Schneider, and J. Nieplocha, "Feasibility studies of applying kalman filter techniques to power system dynamic state estimation," in *Proceedings of the 2007 International Power Engineering Conference (IPEC 2007)*, pp. 376–382, IEEE, Singapore, December 2007.

[8] H. Tebianian and B. Jeyasurya, "Dynamic state estimation in power systems: modeling, and challenges," *Electric Power Systems Research*, vol. 121, pp. 109–114, 2015.

[9] E. Ghahremani and I. Kamwa, "Local and wide-area pmu-based decentralized dynamic state estimation in multi-machine power systems," *IEEE Transactions on Power Systems*, vol. 31, no. 1, pp. 547–562, 2016.

[10] L. Fan and Y. Wehbe, "Extended kalman filtering based real-time dynamic state and parameter estimation using pmu data," *Electric Power Systems Research*, vol. 103, pp. 168–177, 2013.

[11] C. Wang, Z. Qin, Y. Hou, and J. Yan, "Multi-area dynamic state estimation with pmu measurements by an equality constrained extended kalman filter," *IEEE Transactions on Smart Grid*, vol. 9, no. 2, pp. 900–910, 2018.

[12] N. Zhou, D. Meng, Z. Huang, and G. Welch, "Dynamic state estimation of a synchronous machine using pmu data: a comparative study," *IEEE Transactions on Smart Grid*, vol. 6, no. 1, pp. 450–460, 2015.

[13] S. Akhlaghi, N. Zhou, and Z. Huang, "A multi-step adaptive interpolation approach to mitigating the impact of nonlinearity on dynamic state estimation," *IEEE Transactions on Smart Grid*, vol. 9, no. 4, pp. 3102–3111, 2018.

[14] N. Vieyra, P. Maya, and L. M. Castro, "Dynamic state estimation for microgrid structures," *Electric Power Components and Systems*, vol. 48, no. 3, pp. 320–332, 2020.

[15] J. Qi, K. Sun, J. Wang, and H. Liu, "Dynamic state estimation for multi-machine power system by unscented kalman filter with enhanced numerical stability," *IEEE Transactions on Smart Grid*, vol. 9, no. 2, pp. 1184–1196, 2018.

[16] X. Wang, J. Zhao, V. Terzija, and S. Wang, "Fast robust power system dynamic state estimation using model transformation," *International Journal of Electrical Power & Energy Systems*, vol. 114, Article ID 105390, 2020.

[17] N. Zhou, D. Meng, and S. Lu, "Estimation of the dynamic states of synchronous machines using an extended particle filter," *IEEE Transactions on Power Systems*, vol. 28, no. 4, pp. 4152–4161, 2013.

[18] J. Zhao and L. Mili, "Robust unscented kalman filter for power system dynamic state estimation with unknown noise statistics," *IEEE Transactions on Smart Grid*, vol. 10, no. 2, pp. 1215–1224, 2019.

[19] J. Zhao and L. Mili, "A decentralized h-infinity unscented kalman filter for dynamic state estimation against uncertainties," *IEEE Transactions on Smart Grid*, vol. 10, no. 5, pp. 4870–4880, 2019.

[20] Z. Jin, S. Chakrabarti, J. Yu, L. Ding, and V. Terzija, "An improved algorithm for cubature kalman filter based forecasting-aided state estimation and anomaly detection," *International Transactions on Electrical Energy Systems*, vol. 31, no. 5, Article ID e12714, 2021.

[21] N. Vieyra, P. Maya, and L. M. Castro, "Effective dynamic state estimation algorithm for islanded microgrid structures based on singular perturbation theory," *Electric Power Systems Research*, vol. 187, Article ID 106455, 2020.

[22] E. Talebi Ghadikolaee, A. Kazemi, and H. A. Shayanfar, "Multi-area state estimation in a distribution network using takagi-sugeno model estimated by kalman filter," *International Transactions on Electrical Energy Systems*, vol. 30, no. 8, Article ID e12466, 2020.

[23] L. Jiang, Q. Wu, J. Wang, C. Zhang, and X. Zhou, "Robust observer-based nonlinear control of multimachine power systems," *IEE Proceedings - Generation, Transmission and Distribution*, vol. 148, no. 6, pp. 623–631, 2001.

[24] M. A. Mahmud, H. Pota, and M. Hossain, "Full-order nonlinear observer-based excitation controller design for interconnected power systems via exact linearization approach," *International Journal of Electrical Power & Energy Systems*, vol. 41, no. 1, pp. 54–62, 2012.

[25] G. Rigatos, P. Siano, and N. Zervos, "Sensorless control of distributed power generators with the derivative-free nonlinear kalman filter," *IEEE Transactions on Industrial Electronics*, vol. 61, no. 11, pp. 6369–6382, 2014.

[26] J. Qi, A. F. Taha, and J. Wang, "Comparing kalman filters and observers for power system dynamic state estimation with model uncertainty and malicious cyber attacks," *IEEE Access*, vol. 6, pp. 77155–77168, 2018.

[27] N. Vieyra, J. Álvarez, and P. Maya-Ortiz, "Decentralized robust state estimation of multimachine power systems," *International Journal of Electrical Power & Energy Systems*, vol. 135, Article ID 107469, 2022.

[28] J. Alvarez and T. López, "Robust dynamic state estimation of nonlinear plants," *AIChE Journal*, vol. 45, no. 1, pp. 107–123, 1999.

[29] J. Alvarez, "Nonlinear state estimation with robust convergence," *Journal of Process Control*, vol. 10, no. 1, pp. 59–71, 2000.

[30] J. Álvarez and C. Fernández, "Geometric estimation of nonlinear process systems," *Journal of Process Control*, vol. 19, no. 2, pp. 247–260, 2009.

[31] N. Narasimhamurthi, "On the existence of energy function for power systems with transmission losses," *IEEE Transactions on Circuits and Systems*, vol. 31, no. 2, pp. 199–203, 1984.

[32] Q. Lu, Y. Sun, and S. Mei, "Nonlinear excitation control of large synchronous generators," in *Nonlinear Control Systems and Power System Dynamics*, pp. 199–244, Springer, Berlin, Germany, 2001.

[33] M. Galaz, R. Ortega, A. Astolfi, Y. Sun, and T. Shen, "Transient stabilization of multimachine power systems," in *Current Trends in Nonlinear Systems and Control*, pp. 367–386, Springer, Berlin, Germany, 2006.

[34] M. A. Mahmud, M. Hossain, and H. Pota, "Nonlinear excitation controller for power systems using zero dynamic design approach," in *Proceedings of the 2011 North American Power Symposium*, pp. 1–6, IEEE, Boston, MA, USA, August 2011.

[35] M. Mahmud, M. Hossain, and H. Pota, "Transient stability enhancement of multimachine power systems using nonlinear observer-based excitation controller," *International Journal of Electrical Power & Energy Systems*, vol. 58, pp. 57–63, 2014.

[36] M. Mohamed, X.-G. Yan, S. K. Spurgeon, and B. Jiang, "Robust sliding-mode observers for large-scale systems with application to a multimachine power system," *IET Control Theory & Applications*, vol. 11, no. 8, pp. 1307–1315, 2017.

[37] S. Elloumi, B. Abidi, and N. Benhadj Braiek, “Decentralized optimal controller design for multimachine power systems using successive approximation approach,” *Journal of the Franklin Institute*, vol. 350, no. 10, pp. 2994–3010, 2013.
[38] T. Kailath, *Linear systems*, Vol. 156, Prentice-Hall, , Englewood Cliffs, NJ, USA, 1980.
[39] Y. Guo, D. J. Hill, and Y. Wang, “Global transient stability and voltage regulation for power systems,” *IEEE Transactions on Power Systems*, vol. 16, no. 4, pp. 678–688, 2001.
[40] M. A. Mahmud, H. R. Pota, M. Aldeen, and M. J. Hossain, “Partial feedback linearizing excitation controller for multimachine power systems to improve transient stability,” *IEEE Transactions on Power Systems*, vol. 29, no. 2, pp. 561–571, 2014.
[41] J. J. d’Azzo and C. D. Houpis, *Linear Control System Analysis and Design: Conventional and Modern*, McGraw-Hill Higher Education, Columbus, OH, USA, 1995.